Evidence of Anomalous Interaction between a Relativistic Electron Beam and a Solid Target

K. Imasaki, S. Miyamoto, S. Higaki, S. Nakai, and C. Yamanaka
Institute of Laser Engineering, Osaka University, Suita, Osaka, Japan
(Received 9 July 1979)

The dynamic behavior of the plasma produced from a thin foil target irradiated by a focused intense electron beam is observed optically by shadowgraphy and interferometry. Evidence of anomalous stopping of intense electron beam on the surface of the low-z target is shown experimentally.

The investigation of the deposition mechanism of intense relativistic electron-beam (REB) energy to the pellet is an important keypoint for REB inertial-confinement fusion (ICF) research. The size and structure of the pellet for the optimum implosion strongly depend on the energy deposition mechanism of REB electron on the surface of the target. Enhanced energy deposition may reduce the target shell thickness, and the beam energy and power required for breakeven may become much smaller.

Several enhanced-deposition models have been proposed. They are classified into two categories. In model I, by the elongation of the electron path, or a stagnation, in the target due to the magnetic field and/or distorted electric field, the deposition rate of the beam energy is enhanced.[1,2] In this case the transfer mechanism of the beam energy to the target is binary classical collisions in the target of solid density.

In model II, the beam is coupled to the plasma by a hot-beam, two-stream instability which transfers the energy efficiently from the REB to the plasma in the corona region where the growth rate is higher than the collision frequency of the plasma electrons and ions.[3] In this model the characteristic stopping length L may be given roughly as $L \sim \Lambda v_g/\gamma$, where v_g is the group velocity of the wave, Λ is a numerical factor of the order of 10, taking into account the smallness of the initial plasma oscillation, and γ is the growth rate of the instability. γ is described roughly as $\gamma \sim \omega_p(n_b/n_p)$, where ω_p is the plasma frequency, n_p is the plasma electron density, and n_b is the beam electron density.[4] The necessary condition for growth of the plasma wave is described as $\gamma > \nu_{ei}$, where ν_{ei} is the collision frequency of the ions and electrons in the plasma. So the effective energy-deposition region of the REB to the target is in the corona of the plasma where the density is below 10^{20} cm^{-3} and the temperature is several hundred electron volts.

High-Z material is necessary to stop the energetic beam electrons if the deposition process is according to model I. In model II, in contrast, low-Z material is favorable to stop the electrons, because the plasma instability may be suppressed by the higher collision frequency of the higher-Z plasma. In this Letter, experimental evidence for an anomalous deposition in accordance with model II is reported.

The REB generator "Reiden III" was employed to perform the experiment. The typical operating parameters were 500 keV, 100 kA, and 80-nsec pulse length. To enforce the pinching and to get reproducibility in focusing position, a tungsten rod of 1 mm in diameter and 14 mm in height was set at the center of the cathode as shown in Fig. 1. The focal-spot size on the target was 1.05 mm, which is obtained from the high-energy x-ray images in pinhole cameras from the lateral side of the target. The fraction of the focused current to the total diode current was up to 0.8, which was reported elsewhere.[5] The target was set at the bottom of a tapered hole

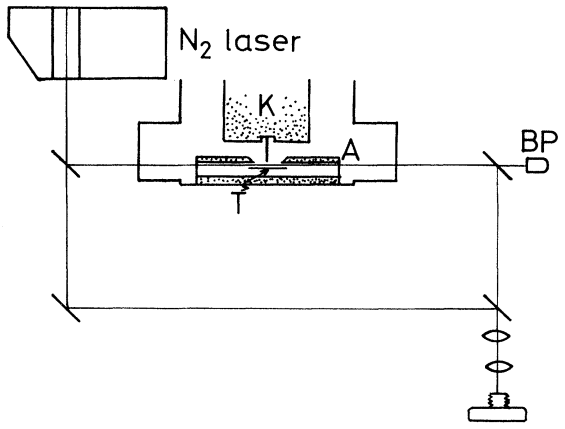

FIG. 1. The schematic description of the interferometry experiment. K is the cathode, A is the anode, and T is the target. The target is suspended from the anode by the brass block which has holes for the path of the light ray.

located at the center of the anode. The diameter of the hole was 20 mm at the top and 10 mm at the bottom, and its depth from the anode surface was 7 mm.

Foils of polyethylene, tantalum, and nickel were used as targets. The targets were suspended by a brass block from the anode. Holes were drilled in the block perpendicular to the beam direction to allow for the laser path and x-ray pinhole camera. The target plasma and its dynamic behavior were measured optically using a N_2 laser of 4-ns pulse width from the horizontal direction along the target surface.

The density profile of the blowoff plasma produced on the front and rear sides of the target was observed by the method of optical interferometry. The expansion velocities of the plasma from the target were measured by two-channel shadowgraphy of successive laser pulses with an optical delay of 25 nsec. The timing of the laser pulse to the voltage pulse was monitored with use of a biplanar photodiode. The experimental setup is shown in Fig. 1 in the case of interferometry measurement.

Typical results of the interferometry for the polyethylene foil of 100 μm in thickness and nickel foil of 10 μm in thickness are shown in Figs. 2(a) and 2(b), respectively. Timing of these pictures is at 100 ns after the voltage pulse rise coinciding with maximum pinch. It is clearly observed for the polyethylene target that the target plasma was expanding only to the front at this time. The density gradient of the rear side still remained in a cold state. Almost the same tendency was obtained even if polyethylene of 25 μm in thickness was used as the target. In the case of a nickel foil target the blowoff of the target occurred equivalently on the front and rear surface.

The classical stopping range for a beam electron of energy several hundred kilo-electron-volts is about 0.1 g cm^{-2}. The values of ρt of the polyethylene foil of 100 μm and the nickel foil of 10 μm in thickness are almost the same and equal to 0.01 g cm^{-2}, where ρ is the mass density and t is the thickness of the target. When the energy deposition is simple classical collisions, the beam electrons penetrate the target of 100-μm polyethylene and 10-μm nickel freely and deposit a small fraction of their energy uniformly over all the volume of the target. Consequently, simultaneous and equivalent blowoff was expected on the front and rear sides of the target of ρt $\sim$ 0.01 g cm^{-2}.

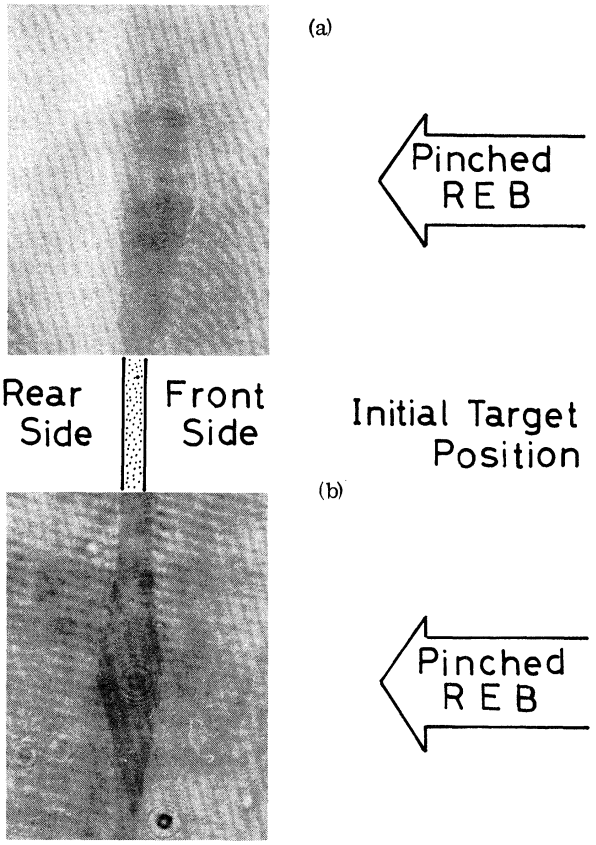

FIG. 2. Typical results for the interferometry: (a) 100-μm polyethylene foil target, (b) 10-μm nickel foil target. Time of results is 100 ns after voltage rise.

In our experiment the effect of the distorted electric field may not play a significant role because the target does not protrude into the diode gap as is considered in model I. The magnetic effect may be conceivable because the skin depth of the field may be comparable to the thickness of the blowoff plasma in the case of Fig. 1 if the plasma temperature is about 10 eV. But the difference of the behavior between the polyethylene and nickel target can not be explained because the ρt of both targets is almost the same.

According to model II, the experimental data could be interpreted as follows. The beam energy may be transferred into the blowoff plasma so efficiently that the beam electrons can not penetrate the target but deposit their energy mainly in the front side of the low-Z target such as polyethylene. So in the case of polyethylene target, the plasma expansion occurred on the front surface while the rear surface remained in a cold state. When a high-Z material such as nickel is

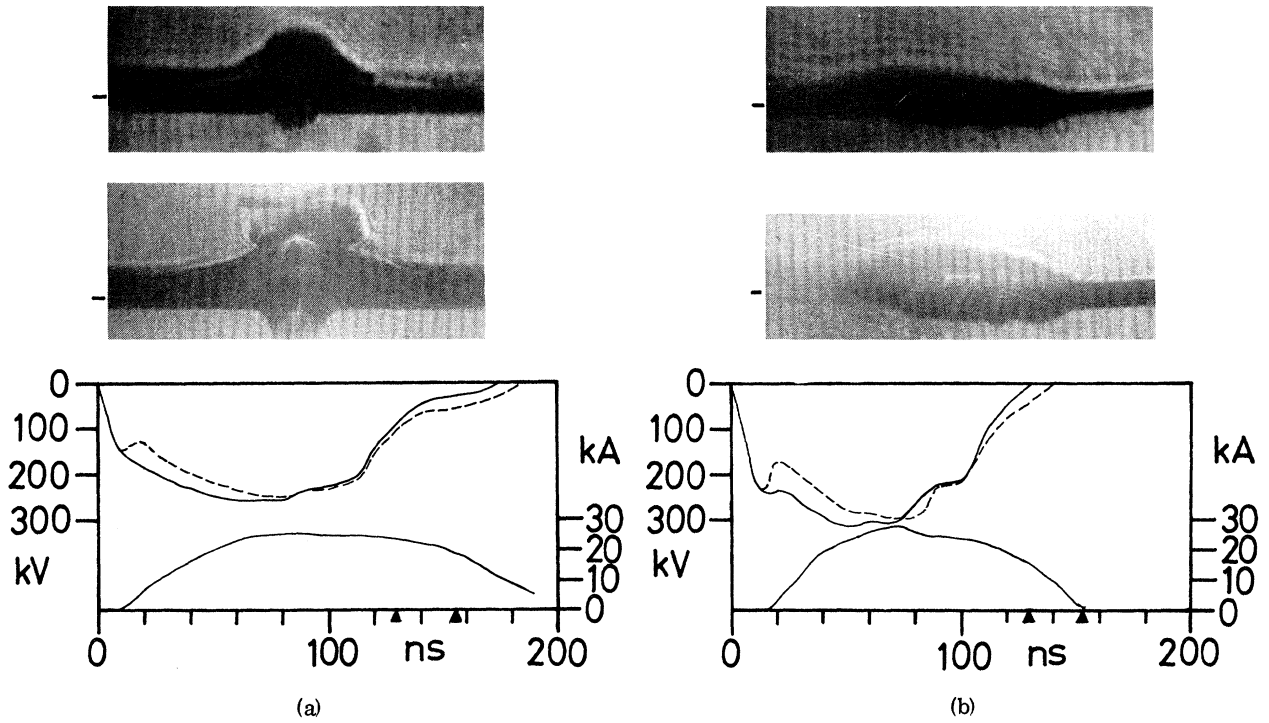

FIG. 3. Typical results for the shadowgraphy with diode voltage and current: (a) 100-μm polyethylene foil target, (b) 20-μm tantalum foil target. Time of results of (a) is 130 ns and 155 ns after voltage pulse rise and (b) is almost the same. Diode voltage wave forms are corrected by $L\,dI/dt$ shown as the broken line.

used for the target, the instability growth may be suppressed due to the strong collisional damping. In the case of the nickel target simultaneous and equivalent expansion of plasma occurred on both sides.

Two successive shadowgrams of the blowoff plasma of the polyethylene of 100 μm in thickness and tantalum of 20 μm in thickness are shown in Figs. 3(a) and 3(b), respectively. Figure 3 also shows the diode voltage and current of each shot. There are no significant differences in the x-ray images between each shot.

The electron density of the plasma at the edge of the shadow was estimated to be about 5×10^{-19} cm^{-3} by comparing with the result of the interferometry. The velocities of the shadow edge obtained from Fig. 3 are shown in Figs. 4(b) and 4(c) by the solid line. For the polyethylene target, from extrapolation of the data for different times, the blowoff occurred only on the front side during the first 100 nsec from the voltage pulse rise. At about 50 nsec after the beginning of the blowoff of the front side, the blowoff of the rear side of the target occurred. This delay of the beginning of the blowoff is explained by the surface absorption of the REB energy, which is also according to model II.

For tantalum foil of 20 μm in thickness the blowoff occurred at almost the same time on both sides. This might be due to the beam penetration through the target, which implied the interaction was the same as in the nickel target.

For the polyethylene target the radius of the plasma on the front side is much larger than that on the rear side. But for the tantalum target, the radii of the plasma on both sides are almost the same. The plasma size on the front side for both targets was much larger than the focal-spot size observed by the x-ray pinhole camera.

This fact is explained as follows. In the case of the tantalum target both sides of the target are heated directly by the penetrating beam so that the plasma of each side produced by thermal conduction along the target surface from the focal spot could have the same size. But for the polyethylene target the beam heats up only the front surface so that the thermal origin on the rear surface may not exist until the thermal wave reaches the rear side.

Behaviors of the blowoff of targets were simu-

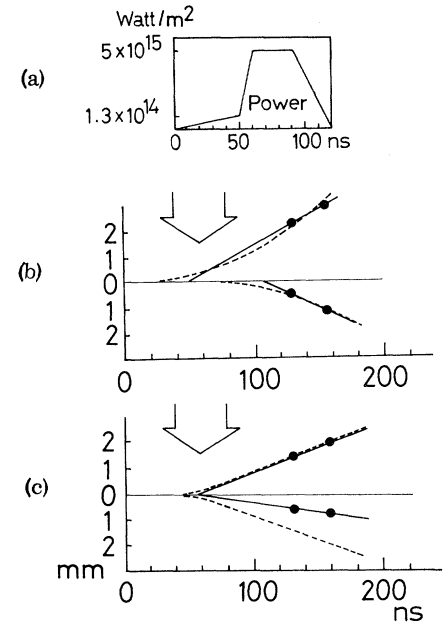

FIG. 4. (a) The incident power for the simulation. (b), (c) The target time history of the experiment and simulation for the polyethylene foil of 100 μm thickness and tantalum foil of 20 μm in thickness, respectively. Solid lines show the experimental result obtained from Figs. 3(a) and 3(b); broken lines show the simulation result.

lated with use of 1-D Lagrangian hydrodynamic code including the self magnetic field which worked as the pressure to the plasma outer edge and beam kinetic pressure. Simulations were performed for the polyethylene foil of 100 μm in thickness and the tantalum foil of 20 μm in thickness. The input power to the target in both cases is shown in Fig. 4(a). This power wave form was determined to fit the power wave forms obtained from the measured diode voltage and current wave form, beam focal-spot size, and pinched beam behavior which are reported elsewhere.[5]

In the simulation for the polyethylene target, 80% of the beam energy deposition was in several outer meshes where a plasma density of 10^{18}–10^{20} cm^{-3} is assumed, which corresponds to model II. For the tantalum target the simulation is performed assuming that 40% of the beam energy is deposited uniformly in the target volume, which corresponds to the simple classical deposition model.

The space-time diagrams of the contour of the plasma of density 5×10^{19} cm^{-3}, as obtained from the simulation, are shown as broken lines in Fig. 4. The simulation results correspond quite well to the experimental results. The blowoff velocities obtained from the experiments as shown in Figs. 4(b) and 4(c) were estimated at the center of the focal spot to minimize the edge effect for comparing with 1-D code. The blowoff velocities of the rear side of the tantalum target obtained from the simulation is two times higher than that obtained from the experiment. This may be due to the profile of deposition of the beam energy which is dissipated during the traveling in the solid target.

Authors wish to thank Dr. K. Nishihara for his helpful discussion about the computer simulation and Mr. Hosokawa and Miss Ohgaki for their help in computer run.

[1]M. J. Clauser, L. P. Mix, J. W. Poukey, J. P. Quintenz, and A. J. Toepfer, Phys. Rev. Lett. 38, 398 (1977).

[2]M. M. Widner, J. W. Poukey, and J. A. Halblieb, Phys. Rev. Lett. 38, 548 (1977).

[3]S. Nakai, K. Imasaki, and C. Yamanaka, in *Proceedings of the Sixth International Conference on Plasma Physics and Controlled Nuclear Fusion Research, Berchtesgaden, West Germany, 1976* (International Atomic Energy Agency, Vienna, 1977).

[4]B. N. Brejzman and D. D. Ryutov, Nucl. Fusion 14, 873 (1974).

[5]S. Miyamoto, K. Imasaki, S. Nakai, and C. Yamanaka, to be published.

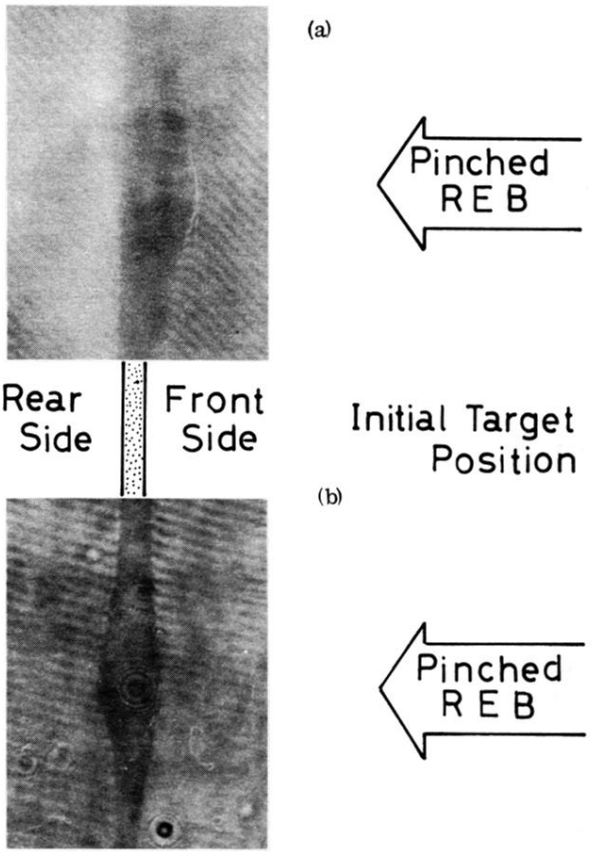

FIG. 2. Typical results for the interferometry: (a) 100-μm polyethylene foil target, (b) 10-μm nickel foil target. Time of results is 100 ns after voltage rise.

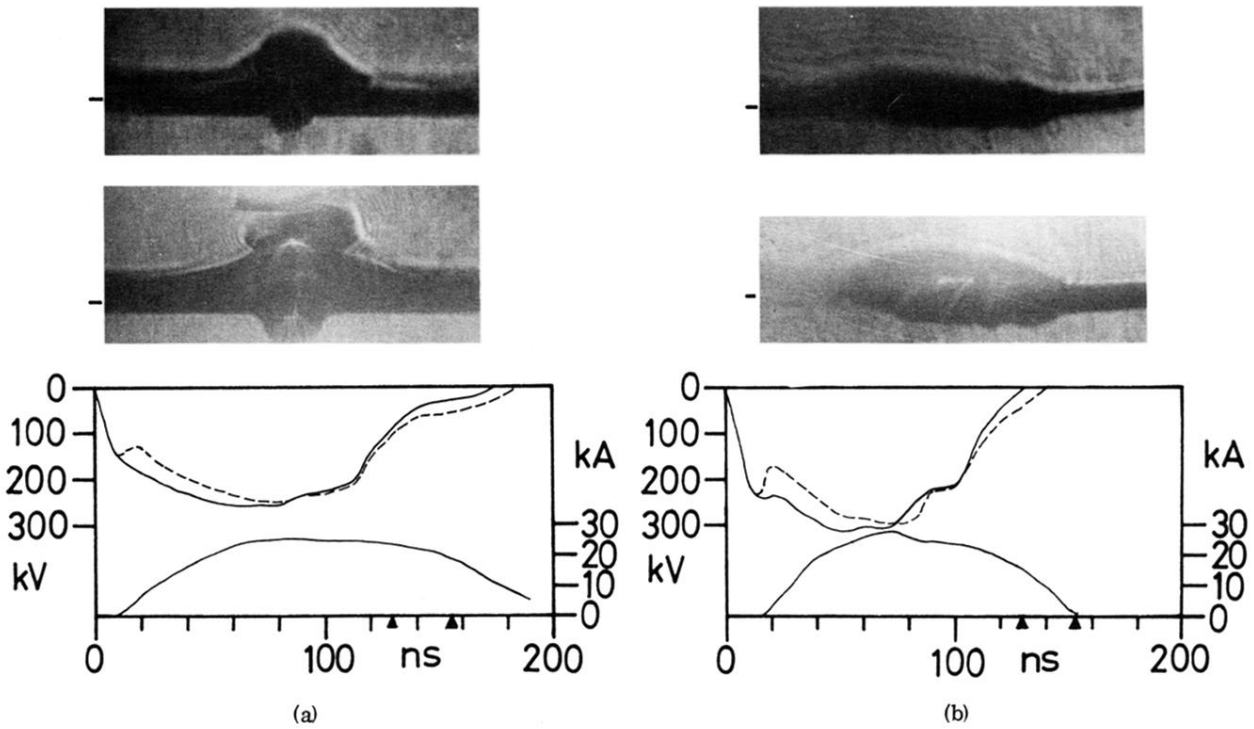

FIG. 3. Typical results for the shadowgraphy with diode voltage and current: (a) 100-μm polyethylene foil target, (b) 20-μm tantalum foil target. Time of results of (a) is 130 ns and 155 ns after voltage pulse rise and (b) is almost the same. Diode voltage wave forms are corrected by $L\,dI/dt$ shown as the broken line.